Indoor mmWave Wearable Networks: Analysis of Interference and Clustering Principles

Yicong Wang and Gustavo de Veciana
Department of Electrical and Computer Engineering, The University of Texas at Austin
Email: yicong.wang@utexas.edu, gustavo@ece.utexas.edu

***Abstract*—Millimeter wave (mmWave) serves as an ideal solution for short range high bandwidth applications in wearable networks. In a dense scenario such as a crowded train or stadium, users are close to each other and the interference can be strong. Furthermore, wearable devices may have heterogeneous transmission capabilities and different Quality-of-Service (QoS) requirements. The wearable network in dense scenarios differs from other mmWave networks in two ways: (1) human body blockage and body movements make interferers have different interfering channels; (2) heterogeneity in device capabilities (e.g. beamforming v.s. omni-directional and different energy constraints) makes it inefficient to schedule all devices in the same way. Different scenarios poses challenges to the design of medium access control (MAC) protocols. In this paper, we begin with an analysis of the characteristics of interferers in dense wearable networks. We compute the number of strong interferers of a typical user and study the stability of strong interferers when users moves locally. We further show that when users make large scale movements, the channel state between two fixed points should be modeled as an $M/G/\infty$ queue instead of two-state Markov model. Based on our analysis of interferers, we discuss the hierarchical MAC to manage interference, including the clustering of users and scheduling at the user level. We propose clustering principles for wearables and analyze the performance of clustering and try to characterize the optimal cluster size of clusters for different scenmarios and device capabilities. We show that coexistence of heterogeneous devices present challenges and clustering and reuse can provide moderate gain in resource reuse but improves the probability of successful transmissions.**

I. Introduction

The market for wearable devices is growing fast in recent years [1] and research on wearable networks is now being actively pursued. In the future, users may be equipped with multiple interconnected devices on the body, some of which may require high bandwidths, e.g., augmented reality devices (other examples required). To support the high data rates and high user densities, millimeter wave communication has been proposed as a possible solution and standards have been developed for short-range wireless personal area network (WPAN) in the mmWave band, e.g., 802.11ad [2], 802.15.3c [3] and ECMA387 [4].

Clearly to be viable, such networks will need to be able to operate in a range of user densities from sparse to very dense ones such as a train cart or a crowded stadium, where the number of interferers is high and existing protocols may fail to coordinate amongst the large number of WPANs so as to meet the QoS requirements of various devices. The design of medium access control (MAC) protocols for dense and heterogeneous wearable networks requires understanding the characteristics of the interference environment and the requirements of different devices.

Related Work Two major factors influencing the interference environment in dense wearable networks are human blockage and user movements. The human body introduces a path loss of over 20dB [6] thus variations in channel gain can be large. The authors in [7] analyze blockage effects in urban areas and model penetration loss of the paths using stochastic geometry. The work in [8] studies human shadowing effects in finite-sized areas when users' locations are fixed. The authors use different path loss exponents and fading models to model the line-of-sight (LOS) and non-line-of-sight (NLOS) channels and approximately compute the signal-to-interference-ratio (SINR) distribution. Subsequently the authors in [9] model the SINR in random networks in an enclosed environment and incorporate the first order reflections off the walls, the ceiling and the floor. The analysis of the interference in the mmWave band has mainly focused on the distribution of SINR where users are assumed to be uncoordinated, i.e., either all users transmit or use simple MAC protocols like Aloha, where they transmit with a given probability.

Another important feature of dense wearable networks is that channels are more sensitive to user movements, including small local movements like turning torso or swinging and large scale movements, e.g., people walking around. Existing work on the user mobility includes [10][11][12], which study the influence of human mobility on the radio channel between fixed transmitter and receiver. The authors of [10][12] present measurements of the impact of human mobility on channel variations. The work in [12] further computes the probability that a channel is blocked by users and model the state of channel using a two-state Markov model. Authors of [11] use simulations to get the radio propagation characteristics in the presence of static and moving obstacles and show that directional LOS wave links experience relatively high outage. These works provide valuable measurements and insights on the influence of moving human blockage, but they do not provide tractable analysis of user movements to quantify the influence of user mobility.

In dense wearable networks, the MAC protocol needs to coordinate users' transmissions to improve the reuse of the resources and ensure application QoS. Many existing works on MAC design focus on improving resource reuse for centralized networks where a single Piconet Coordinator (PNC) (in 802.15.3c) or Access Point (AP) (in 802.11ad) coordinates

the transmissions of different links [13][14][15]. Only the interference within the Piconet / Basic Service Set (BSS) is considered while the interference among different networks is neglected. Centralized MACs require signaling overheads for measurement and control signals. In dense wearable networks, the channel between different users are unreliable and the number of devices/BSSs may be large, thus existing works on centralized MAC may fail to schedule the devices. The authors of [16][17] study distributed MAC protocols for mmWave networks and use memory to improve the resource reuse of the system. However, in highly dense wearable networks, the number of potential interferers can be high and pure distributed MAC may fail to efficiently coordinate amongst the large numbers of users.

The 802.11ad standard provides a hierarchical MAC geared at coordinating the personal basic service sets (PBSSs). The devices of a user forms a PBSS with a device working as the PBSS coordinate point (PCP). PCPs may use the PCP clustering mechanism to improve the spatial sharing and interference mitigation with other co-channel directional multi-gigabit (DMG) BSSs. Multiple PBSSs form a cluster, with one PCP/AP selected as the synchronization PCP (S-PCP), which can be viewed as the cluster head. There are two types of clustering, decentralized PCP/AP clustering and centralized PCP/AP clustering. Centralized clustering requires synchronization and coordination of multiple S-APs, which might be hard to achieve in wearable networks where users might moves and the channel between distant PCPs can be unstable. In this paper, we focus on the decentralized clustering. In decentralized clustering, the S-PCP synchronizes the PCPs in the cluster and schedules beacon transmissions of each PCP while the PCPs schedule the data transmission for each BSS. To avoid interference, a PCP may re-schedule service periods (SPs) and contention-based access periods (CBAPs) in its beacon interval or move the beacon transmission interval in an attempt to mitigate any interference with transmission indicated in the received Extended Schedule element in the beacons of other BSSs. The BSSs work in a TDMA-like scheme but the resources allocated to each BSS may not be enough. In dense wearable networks, the channels are unstable due to human blockage and movements, and so clusters may suffer from frequent changes in topology. The problem of selecting the channel and the cluster to join when multiple clusters are available is not specified. In this paper, we propose principles for clustering and channel selection based on our analysis of mmWave environment.

Paper Contributions In this paper, we address the MAC design in dense indoor mmWave wearable networks. We consider the case where the user density is high and the devices on a user form a BSS coordinated by the smart phone. Due to the high density of users and unstable channels, the measurements of channel and the exchange of signaling is limited thus the MAC should rely on limited channel measurements and be robust to changes in network topology and we aim to propose the principles of MAC for such network.

We first provide an analysis of the mmWave interference environment, specifically, we characterize the set of strong interferers (SIs) a BSS might see in a dense wearable network. We define strong interferers of a user as other users whose PCPs have a strong channel to the PCP of the target user. We model the users as a marked point process (m.p.p.) with the locations of the users following a Poisson Point Process (PPP) and the orientations of the users captured by marks. We compute the spatial distribution of strong interferers and show that the number of strong interferers is limited as user density increases. We then analyze the influence of user movements of different scales, i.e., small local movements and large scale constant velocity movements. For small local movements, we compute the sensitivity of strong interferers at different distances and show that strong interferers are most sensitive when user density is moderately high, assuming that the range of local movements is limited for high user density. For large scale movements, we assume that users move at constant velocities and analyze the channel state of a fixed link. We prove that the blockage state of the channel follows an alternating renewal precess which is not quite the simple Markov model used in existing works and the distribution of length of the blocked period is different from exponential distribution. We further compute the average length of intervals of channel being clear or blocked using the analytical model.

Based on our analysis of strong interferers, we argue that clustering plus MAC scheduling at BSS is a viable hierarchy for dense wearable networks. Clustering and channel selection can be used to mitigate interference while scheduling at each user can be used to schedule wearable devices and improve channel reuse by learning the transmission patterns of other users. We propose a clustering and channel selection algorithm based on Affinity Propagation (AP) and show that the proposed algorithm can improve the stability of channels between cluster members and cluster heads and reduce inter-cluster interference.

Thirdly, we propose a simple model to analytically evaluate the performance of clustering and channel selection for dense wearable networks with heterogeneous devices, i.e., transmission capabilities and traffic demands. The members of a cluster are randomly distributed in a disc, whose size depends on the cluster size, and its cluster head is located at the center of the circle. The benefir of frequency division across clusters is modeled as a ring protection region around the cluster. The size of the protection region depends on the cluster size and the number of channels. Interferers are randomly located outside of the protection region following a thinned P.P.P.. Users within the same cluster can coordinate with each other and achieve full spatial reuse while the interferers outside the cluster are not synchronized and there is no coordination among clusters. Using our proposed model, we are able to compute the successful transmission time (STT) for different user densities and user devices. We can also study the optimal cluster size maximizing average STT for different scenarios. Our results indicate that clustering and reuse provide moderate gains in STT due to beacon overheads but improve the probability of

successful transmission.

The rest of the paper is organized as follows. In the next section, we give the analysis of the strong interferers and how user movements affect the interference environment using stochastic geometry tools. We present the numerical results of the analysis and discuss their implications on MAC design in Section III. In Section IV, we discuss the clustering and channel selection principles and propose AP-based clustering algorithm. In Section V we analyze the performance of clusters for different scenarios and characterize the optimal cluster size. Section VI concludes our paper.

II. Interference in Dense Wearable Network

In a highly dense wearable network, a user may have a large number of neighbors in close proximity, but there are several factors limiting the actual number of interferers a user sees, including the shadowing by the human body, environmental obstructions and the directionality of transmissions, which might further be enhanced by the upward-downward directionality of wearable applications. Also, directional transmissions limit the width of transmission beams thus a user will be interfering with fewer other users. The upward-downward directionality results from the typical posture of humans and locations of common wearable devices. Many devices are located along the torso instead of around the torso thus when directional transmissions are used, transmission is in upward or downward direction, reducing the likelihood of interfering with other users.

The precise modeling of mmWave channels, especially the NLOS channels is still an open question and there has been much effort towards developing channel models based on measurements. In our analysis, we shall focus on two salient characteristics, human body blockage of interference and one time reflection on the ceiling. We ignore reflections or scattering from human bodies or other objects.

A. System Model for Wearable Network

We consider a wearable network of PBSSs, each consists of the wearable devices on a user and study the interference environment seen by a typical user. Suppose users are standing on a 2-D plane. There is no walls or obstructions other than human bodies, and there is a ceiling at a height of h_{ceiling} meters.

For simplicity, we assume the locations of PCPs on the human body are the same and the users' bodies are of the same dimensions. Users are of the same height, h_{body} and the cross section of human body at h_{device} is a convex shape A. The PCPs are located in front of user bodies at a height of h_{device}. In this way, user i, u_i, can be decided by his location x_i and orientation θ_i. We assume x_i's follow a point process $\Phi = \{x_i\}_i$ and the orientation of user i is θ_i. The network can be modeled as a marked point process (m.p.p.) $\tilde{\Phi} = \{(x_i, \theta_i)\}_i$. The typical user u_0 is located at the origin, $x_0 = 0$, and the orientation is θ_0.

We use the link between the centers of two users to approximate the actual channel between the PCPs. Denote the line-of-sight (LOS) channel between u_0 and user located at x as $l_{0,x}^{\text{LOS}}$ and the non-line-of-sight (NLOS) reflected channel over the ceiling as $l_{0,x}^{\text{NLOS}}$. The path loss of $l_{0,x}^{\text{LOS}}$ follows the free space propagation, $L = 20\log_{10}\left(\frac{4\pi l}{\lambda}\right)$. For $l_{0,x}^{\text{NLOS}}$, the path loss is decided by the length of the pass and the reflection coefficient, which is decided by the material and incident angle. User centered at x is a strong interferer if either LOS or NLOS channel is not blocked and has a low path loss. The path loss is below the threshold if

$$r_{0,x} < r_{\max} \tag{1}$$

for LOS channel, and

$$r_{0,x} < r_{\max}^{\text{reflection}} \tag{2}$$

for reflected channel, where $r_{0,x}$ is the distance between the centers of the users. $r_{\max}$ is the max distance of a LOS strong interferer and $r_{\max}^{\text{reflection}}$ is the maximum distance of a reflected strong interferer, which is related to h_{ceiling}, h_{device} and material of the ceiling. Notice that the reflection coefficient may not be a monotonic function of incident angle [18]. It is possible that a distant user might have a stronger reflection channel than a close user, thus $\{r_{0,x} < r_{\max}^{\text{interference}}\}$ may not be the sufficient condition to decide whether the path loss is below the threshold. In this paper, we stick to the simple condition in (1) and (2), but our results can be easily extended to incorporate different reflection models.

B. Number of Strong Interferers

We first analyze the set of strong interferers seen by a typical user. Using our system model, the number of strong interferers seen by the typical user, N_{SI} is given by,

$$N_{\text{SI}}(\tilde{\Phi}, \theta_0) = \sum_{(x_i,\theta_i)\in\tilde{\Phi}} f_0(x_i, \theta_i, \tilde{\Phi}\backslash\{(x_i,\theta_i)\}, \theta_0) \tag{3}$$

where $f_0(x_i, \theta_i, \tilde{\Phi}\backslash\{(x_i,\theta_i)\}, \theta_0)$ is the indicator function that u_i located at x_i and with orientation θ_i is a strong interferer of the typical user located at the origin. Note this depends on blockages from other users, i.e., $\tilde{\Phi}\backslash\{(x_i,\theta_i)\}$. f_0 is 1 if there is a strong LOS channel between devices or a strong unblocked reflected channel over the ceiling.

N_{SI} depends on realization of $\tilde{\Phi}$, making the distribution of N_{SI} hard to compute. Still the average number of strong interferers is a good metric to understand the coordination requirements of MAC. Assuming that $\{\theta_i\}$ are mutually independent and the distribution of θ_i depends only on the location of the user, x_i, then $\tilde{\Phi}$ is independently marked point process (i.m.p.p.) [19]. Given these assumptions, we can compute the expected number of strong interferers in the following theorem.

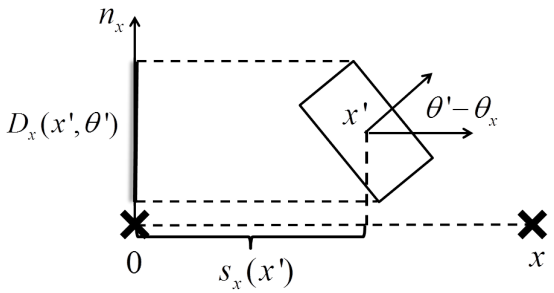

Fig. 1. User (x',θ') will block the LOS channel between 0 and x if the projection of x' lies on x and the projection of his cross-segment covers 0.

Theorem 1. *$\tilde{\Phi}$ is an i.m.p.p., then $\mathrm{E}[N_{\mathrm{SI}}]$ is given y,*

$$\begin{aligned}\mathrm{E}[N_{SI}] &= \mathrm{E}^0\Big[\int\limits_{\mathbb{R}^2\times[0,2\pi)} f_0(x_i,\theta_i,\tilde{\Phi}\backslash\{(x_i,\theta_i)\},\theta_0)\tilde{\Phi}(\mathrm{d}(x,\theta))\Big]\\ &= \int\limits_{\mathbb{R}^2}\int\limits_{[0,2\pi)}\int\limits_{\tilde{\mathbb{M}}} \mathrm{E}_{\theta_0}[f_0(x,\theta,\tilde{\phi},\theta_0)]P^!_{(x,\theta)}(\tilde{\phi})F_x(\mathrm{d}\theta)M(\mathrm{d}x)\end{aligned} \tag{4}$$

Proof. Theorem 1 follows the Reduced Campbell's formula for i.m.p.p. of Corollary 2.2 in [19], by taking expectation over θ_0 and use $\mathrm{E}_{\theta_0}[f_0(x,\theta,\tilde{\phi},\theta_0)]$ as the non-negative function defined on $\mathbb{R}^2\times\mathbb{R}\times\tilde{\mathbb{M}}$. □

In Theorem 1, E^0 is the expectation given that there is a user at the origin, E_{θ_0} is the expectation over θ_0, $\tilde{\mathbb{M}}$ is the set of all possible realizations of $\tilde{\Phi}$, $P^!_{(x,\theta)}$ is the Palm distribution of marked point process given that there is a point (x,θ) and a point at the origin. $F_x(\mathrm{d}\theta)$ is the probability measure of the orientation of the user located at x and $M(S)=\mathrm{E}[\Phi(S)]$ is the mean measure of the points Φ.

For tractability, we use homogeneous Poisson Point Process (HPPP) to model the locations of users, and the density of the HPPP is λ. For the channel between the typical user and a user located at x, other users are uniformly distributed over $\mathbb{R}^2\backslash\{0,x\}$. We also assume that the facing directions of users are independent of user locations and uniformly distributed in $[0,2\pi)$. A user (x',θ') blocks if the projection of x' on $l^{\mathrm{LOS}}_{0,x}$) lies on the segment between 0 and x, $s_x(x')\in[0,|x|]$, and the cross section of user body projection on n_x does not cross the origin 0, see Fig. 1. $s_x(x')$ is the projection of x' on x, n_x is the unit vector perpendicular to x and $D_x(x,\theta')$ is the projection of user's cross-section on n_x. Based on the geometric analysis, we can compute the probability that a user located at x is a strong interferer of the typical user.

Theorem 2. *The number of users blocking $l^{\mathrm{LOS}}_{0,x}$, $N^{\mathrm{LOS}}_{\mathrm{B}}(x)$, follows Poisson distribution and the average number of blockage $\mathrm{E}[N^{\mathrm{LOS}}_{\mathrm{B}}(x)]\approx\lambda|x|\mathrm{E}[D]$. $\mathrm{E}[D]$ is the expected width of cross section of user.*

Proof. The number of blockages is given by,

$$N^{\mathrm{LOS}}_{\mathrm{B}}(x)=\sum_{(x_i,\theta_i)\in\tilde{\Phi}\backslash(x,\theta)} 1\big((x_i,\theta_i)\text{ blocks }l^{\mathrm{LOS}}_{0,x}\big).$$

$\tilde{\Phi}\backslash(x,\theta)$ is an independently marked PPP and $1\big((x_i,\theta_i)\text{ blocks }l^{\mathrm{LOS}}_{0,x}\big)$ only depends on (x_i,θ_i). $N_{\mathrm{B}}(x)$ is an independently thinned Poisson process, which is still a Poisson process [19].

$$\begin{aligned}\mathrm{E}[N^{\mathrm{LOS}}_{\mathrm{B}}(x)] &= \int\limits_{\mathbb{R}^2}\int\limits_{[0,2\pi)} 1((x',\theta')\text{ blocks }(x,\theta))F_{\theta'}(\mathrm{d}\theta')\lambda(\mathrm{d}x')\\ &\overset{(a)}{\approx} \int\limits_{\mathbb{R}^2}\int\limits_{[0,2\pi)} 1\big(0\notin D_x(x',\theta')\big)\\ &\qquad\times 1\big(s_x(x')\in[0,|x|]\big)F_{\theta'}(\mathrm{d}\theta')\lambda(\mathrm{d}x') \qquad (5)\\ &\overset{(b)}{=} \lambda|x|\int\limits_{[0,2\pi)}|D_x(\cdot,\theta')|F_{\theta'}(\mathrm{d}\theta')\\ &\overset{(c)}{=} \lambda|x|\mathrm{E}[|D_x|] \qquad (6)\end{aligned}$$

where in (a), we use the two conditions of projections to approximate $1((x',\theta')\text{ blocks }(x,\theta))$. In (b), we use the fact that users follows HPPP with density λ. The location the dimensions of users are independent of the locations of users thus the distribution of $|D_x(x',\theta')|$ is independent of x'. In (c), $\mathrm{E}[|D_x|]$ is the expectation of B_x over user orientations. If the orientations of users is uniform over $[0,2\pi)$, then $\mathrm{E}[|D_x|]$ is the same for all x. Denote $\mathrm{E}[D]=\mathrm{E}[|D_x|]$ and this finishes the proof. □

By Theorem 2, the probability that $l^{\mathrm{LOS}}_{0,x}$ is blocked over $\tilde{\mathbb{M}}$ is given by $e^{-E[N^{\mathrm{LOS}}_{\mathrm{B}}(x)]}$. For LOS channel, f_0 can be written as,

$$\begin{aligned}f_0(x,\theta,\tilde{\phi},\theta_0)=1((x,\theta)\text{ faces }(0,\theta_0))\cdot 1(N^{\mathrm{LOS}}_{\mathrm{B}}(x)=0)\\ \cdot 1(|x|\le r_{\max}).\end{aligned} \tag{7}$$

Based on our assumption on user locations and orientations, we can compute $\mathrm{E}[N^{\mathrm{LOS}}_{\mathrm{SI}}]$ as follows,

$$\begin{aligned}\mathrm{E}[N^{\mathrm{LOS}}_{\mathrm{SI}}] &= \int\limits_{\mathbb{R}^2\backslash\mathrm{B}(0,r_{\min})}\int\limits_{[0,2\pi)} \mathrm{E}_{\theta_0}[1((x,\theta)\text{ faces }(0,\theta_0))]\\ &\qquad\cdot 1(|x|\le r_{\max})\cdot e^{-\mathrm{E}[N^{\mathrm{LOS}}_{\mathrm{B}}(x)]}F_\theta(\mathrm{d}\theta)\lambda(\mathrm{d}x)\\ &\overset{(a)}{=} \int\limits_{\mathbb{R}^2\backslash\mathrm{B}(0,r_{\min})}\mathrm{P}_{\text{facing}}(x)1(|x|<r_{\max})e^{-\mathrm{E}[N^{\mathrm{LOS}}_{\mathrm{B}}(x)]}\lambda(\mathrm{d}x)\\ &= 2\pi\lambda\mathrm{P}_{\text{facing}}\int\limits_{r_{\min}}^{r_{\max}} e^{-\lambda\cdot\mathrm{E}[D]\cdot r}r\mathrm{d}r\\ &= \frac{2\pi\mathrm{P}_{\text{facing}}}{\lambda\mathrm{E}[D]^2}\big(e^{-\lambda\mathrm{E}[D]r_{\min}}(\lambda\mathrm{E}[D]r_{\min}+1)\\ &\qquad - e^{-\lambda\mathrm{E}[D]r_{\max}}(\lambda\mathrm{E}[D]r_{\max}+1)\big)\end{aligned} \tag{8}$$

In (a), $\mathrm{P}_{\text{facing}}$ is the probability that the link is not blocked by the typical user or the user (x,θ), i.e.,

$$\mathrm{P}_{\text{facing}}(x)=\int\limits_{[0,2\pi)}\mathrm{E}_{\theta_0}[1((x,\theta)\text{ faces }(0,\theta_0))]F_\theta(\mathrm{d}\theta)$$

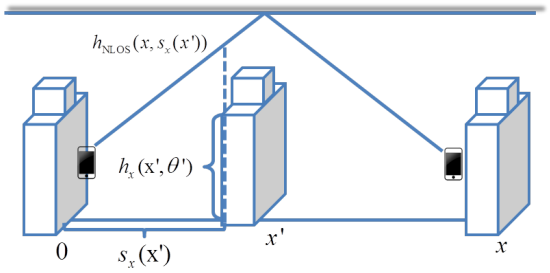

Fig. 2. User x has a clear reflected channel if there is no other user blocking the reflection path, i.e., there is no user (x', θ') such that $\{s_x(x') \in [0, |x|]\} \cap \{h_x(x', \theta') \geq h_{\text{NLOS}}(x, s_x(x'))\}$.

We assume that user orientations are uniform over $[0, 2\pi)$, thus $\mathrm{P}_{\text{facing}}(x)$ is same for all x and we use $\mathrm{P}_{\text{facing}}$ as the probability of the two users are not blocked by the bodies of the typical user and the potential interferer. $r_{\min}$ is the minimum distance between the centers of the users.

For NLOS channel, the number of blockages also follows Poisson distribution. We can compute $\mathrm{E}[N_{\mathrm{B}}^{\mathrm{NLOS}}]$ in a similar way as above for $\mathrm{E}[N_{\mathrm{B}}^{\mathrm{LOS}}(x)]$ by substituting the first indicator function in (5), $1\big(0 \notin B_x(x', \theta')\big)$, with

$$1\big(h_x(x', \theta_{x'}) > h_{\text{NLOS}}(x, s_x(x'))\big),$$

where $h_x(x', \theta_{x'})$ is the height of user of x' along x. $h_{\text{NLOS}}(x, s_x(x'))$ is the height of the reflection channel as shown in Fig. 2.

We make further assumptions about users that user bodies are cylinders, or more generally, the cross section of user body at height h_1, $\sigma(h_1)$, is contained in the cross section of user body at height h_2, $\sigma(h_2)$, for $h_1 \geq h_2 \geq h_{\text{device}}$, i.e.,

$$\sigma(h_1) \subseteq \sigma(h_2), \forall h_1 \geq h_2 \geq h_{\text{device}}. \tag{9}$$

If the users satisfies the condition in (9), a user that does not block $l_{0,x}^{\mathrm{LOS}}$, i.e., $x \cap \sigma(h_{\text{device}}) = \emptyset$, then $x \cap \sigma(h') = \emptyset$ for $h' > h_{\text{device}}$, indicating that the user will not block the reflected channel $l_{0,x}^{\mathrm{NLOS}}$.

Combining the above results, the expected number of strong interferers is given by

$$\begin{aligned}\mathrm{E}[N_{\mathrm{SI}}] = \int_{\mathbb{R}^2} & \mathrm{P}_{\text{facing}}(x) \\ & \cdot \Big[1(|x| \in [r_{\min}, r_{\max}^{\text{reflection}}]) \cdot e^{-\mathrm{E}[N_{\mathrm{B}}^{\mathrm{NLOS}}(x)]} \\ & + 1(|x| \in [r_{\max}^{\text{reflection}}, r_{\max}]) \cdot e^{-\mathrm{E}[N_{\mathrm{B}}^{\mathrm{LOS}}(x)]}\Big] \lambda(\mathrm{d}x)\end{aligned} \tag{10}$$

C. Sensitivity of Strong Interferers

In this section we introduce local movements model and study the sensitivity of strong interferers to user's small local movements. Interference channels are sensitive to user movements, especially for dense wearable networks. The sensitivity of strong interferers defines the cost and benefit of keep tracking of and coordinating the strong interferers and how robust the strong interferers are to perturbations in the network. Suppose in a time interval $[t, t + \Delta t]$, users make translations as well as rotations, resulting in changes for the typical user and potential interferers summarized as follows:

$$\begin{aligned}(0, \theta_0) &\to (\Delta x_0, \theta_0 + \Delta\theta_0) \\ \tilde{\Phi}^t = \{(x_i, \theta_i)\} &\to \tilde{\Phi}^{t+\Delta t} = \{(x_i + \Delta x_i, \theta_i + \Delta\theta_i)\}\end{aligned}$$

Let $Y_x^t = f_0(x, \theta, \tilde{\Phi}^t \backslash (x, \theta), \theta_0)$ be the state of the interferer located at x at time t, and $Y_x^{t+\Delta t}$ be the state of the same user at $t + \Delta t$, which is given by,

$$\begin{aligned}Y_x^{t+\Delta t} = f_{\Delta x_0}(x + \Delta x, \theta + \Delta\theta, \tilde{\Phi}^{t+\Delta t} \backslash (x + \Delta x, \theta + \Delta\theta), \\ \theta_0 + \Delta\theta_0),\end{aligned}$$

Y_x^t and $Y_x^{t+\Delta t} \in \{0, 1\}$. $Y = 1$ if the user is a strong interferer of the typical user and $Y = 0$ otherwise. We define the sensitivity of an interferer originally located at x, $S(x)$, via the autocorrelation of the state of the interferer at t and $t + \Delta t$. We define $S(x, \Delta t)$ as follows,

$$S(x, \Delta t) = \mathrm{Corr}(Y_x^t, Y_x^{t+\Delta t}) = \frac{\mathrm{E}[Y_x^t \cdot Y_x^{t+\Delta t}]}{\sigma_{Y_x^t} \cdot \sigma_{Y_x^{t+\Delta t}}}. \tag{11}$$

By definition of $S(x, \Delta t)$ and the range of Y_x, we have $S(x, \Delta t) \in [0, 1]$. If $S(x, \Delta t)$ is small, the autocorrelation between the state of the channel is small and sensitive to movements; if $S(x, \Delta t)$ approximates 1, the autocorrelation is high and the strong interferer is stable.

We assume the locations of users follow HPPP of density λ and the users make movements independent of their locations. For the orientations of users, we assume $\tilde{\Phi}$ is i.m.p.p. and $\theta \sim \mathrm{unif}(0, 2\pi)$, also the rotation of users is independent of users' orientations.

To compute $S(x, \Delta t)$, we need to know the distribution of users in presence of movements. We assume users are uniformly distributed on the plane and users make independent movements, then we have the following theorem on the Φ.

Theorem 3. *If Φ^t is HPPP with density λ and users make independent movements and the movements is indepedent of users' location, then $\Phi^{t+\Delta t}$ is still HPPP with density λ.*

Proof. Let $p_{t,t+\Delta t}(x, x + \Delta x)$ be the probability that the user located at x at time t moves to $x + \Delta x$ at time $t + \Delta t$. Users' movements are independent and the movements are independent of x, then $p_{t,t+\Delta t}(x, y)$ is a function of Δx, i.e., $p_{t,t+\Delta t}(x, x + \Delta x) = g_{t,t+\Delta t}(\Delta x)$. According to the displacement theorem in [23], $\Phi^{t+\Delta t}$ is a HPPP with density λ. □

Based on our assumptions on user movements and orientation, we have the following theorem for $\tilde{\Phi}$.

Theorem 4. *$\tilde{\Phi}^{t+\Delta t}$ is an i.m.p.p. and θ is uniform in $[0, 2\pi)$ at $t + \Delta t$.*

Proof. θ and $\Delta\theta$ are independent from other users and the locations and translations of users, x and Δx, thus $\tilde{\Phi}^{t+\Delta t}$ is i.m.p.p.. If $\theta^t \sim \mathrm{unif}(0, 2\pi)$ and $\Delta\theta$ is independent from θ^t, then follow the similar proof used in displacement theorem, $\theta^{t+\Delta t} \sim \mathrm{unif}(0, 2\pi)$. □

By Theorem 3 and 4, $\tilde{\Phi}$ is stationary thus the variance of Y_x^t and $Y_x^{t+\Delta t}$ are the same and independent of t or Δt,

$$\mathrm{Var}(Y_x) = p_{\mathrm{SI}}(x) \cdot (1 - p_{\mathrm{SI}}(x)),$$

where $p_{\mathrm{SI}}(x) = \Pr(f_0(x, \theta, \tilde{\Phi} \backslash \{(x_i, \theta_i)\}, \theta_0) = 1)$.

By definition,

$$\mathrm{E}[Y_x^t \cdot Y_x^{t+\Delta t}] = \Pr(\{Y_x^t = 1\} \cap \{Y_x^{t+\Delta t} = 1\}),$$

is the probability that user at x is strong interferer at t and $t + \Delta t$. The movements of users during Δt, $(\Delta x, \Delta\theta)$ can be counted as marks of Φ, and the new m.p.p. is $\tilde{\Phi}^{\Delta t} = \{(x_i, m_i)\}_i$, where $m_i = (\theta_i, \Delta x_i, \Delta\theta_i)$ is the new marks of the point process. According to our assumptions of independently marked process, $\tilde{\Phi}^{\Delta t}$ is an i.m.p.p..

Denote $f_0^{\Delta t}(x_i, m_i, \tilde{\Phi}^{\Delta t} \backslash (x_i, m_i), m_0)$ be the indicator function that the user located at x is a strong interferer at t and $t + \Delta t$, then

$$\begin{aligned} f_0^{\Delta t}(x_i, m_i, \tilde{\Phi}^{\Delta t} \backslash (x_i, m_i), m_0) = \\ f_0(x, \theta, \tilde{\Phi}, \theta_0) \cdot f_{\Delta x_0}(x + \Delta x, \theta + \Delta\theta, \\ \tilde{\Phi} + \Delta\tilde{\Phi} \backslash (x + \Delta x, \theta + \Delta\theta), \theta_0 + \theta_0), \end{aligned}$$

where $\Delta\tilde{\Phi} = \{(\Delta x_i, \Delta\theta_i)\}_i$ is the movement of users during Δt and we denote $\tilde{\Phi} + \Delta\tilde{\Phi} = \{(x_i + \Delta x_i, \theta_i + \Delta\theta_i)\}_i$ as the network after users move. Given the model of movements, i.e., $F_{(\Delta x, \Delta\theta)}$, we can compute $\mathrm{E}[f_0^{\Delta t}]$ using the same technique used in the previous section.

D. Influence of Mobile Blockers on Static Wearable Networks

Another scenario we are interested in is dense user environment where some users move and the other users stay fixed, e.g., in a train cart, some users are sitting in their seats while other users are leaving the train through the passage. In this section we study the influence of mobile blockers on static channels. We assume the blockers make constant velocity movements towards their orientation and we refer to the model as Constant Velocity Model(CVM).

We first introduce the following operations on subsets in $A, B \in \mathbb{R}^d$,

$$\begin{aligned} A \oplus B &= \{x + y : x \in A, y \in B\}, \\ x + B &= \{x + y : y \in B\}, \text{ for } x \in \mathbb{R}^d, \\ \check{B} &= \{x : -x \in B\}. \end{aligned}$$

Now we describe the assumptions about CVM in detail. At time 0, the locations of users, $\Phi^0 = \{x_i^0\}_i$, follows HPPP with density λ, and the orientations of users is independently and uniformly distributed in $[0, 2\pi]$, $\theta_i \sim \mathrm{unif}(0, 2\pi)$. Users moves towards their orientation at constant speeds $\{s_i\}_i$ and s_i's are independently and identically distributed (i.i.d.).

Let $A_0^{\theta_i}$ be the cross-section of user centered at 0 facing θ_i. $A_0^{\theta_i}$ is convex and bilateral symmetrical along θ_i. x_i^t is the location of the center of u_i at time t, then the area u_i blocks at time t, $A_{x_i}^t$, is given by

$$A_{x_i}^t = x_i^t + A_0^{\theta_i}.$$

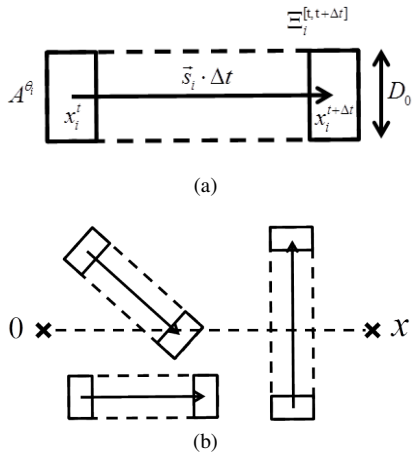

Fig. 3. (a) shows the $\Xi_i^{[t,t+\Delta t]}$. If $A_0^{\theta_i}$ is convex then Ξ is also convex. In (b) u_i blocks channel in $[t, t + \Delta t]$ if $\Xi_i^{[t,\Delta t]} \cap x \neq \emptyset$.

From t to $t+\Delta t$, u_i moves from x_i^t to $x_i^{t+\Delta t} = x_i^t + \vec{s}_i \cdot \Delta t$ and we denote the $l_{x_i^t, x_i^{t+\Delta t}}$ as the trace of the center of u_i. The area that u_i covers during $[t, t + \Delta t]$, $\Xi_i^{[t,t+\Delta t]}$, is as follows,

$$\Xi_i^{[t,t+\Delta t]} = A_0^{\theta_i} \oplus l_{x_i^t, x_i^{t+\Delta t}}.$$

Fig. 3 illustrates the boolean model of mobile blockages.

The distribution of user locations and velocities is given in the following theorem.

Theorem 5. *Suppose users make i.i.d. constant speed movements and the locations of users follows HPPP at time* 0*, then* $\tilde{\Phi}_c^t = \{(x_i^t, (\theta_i, s_i))\}_i$ *is stationary.*

The proof uses displacement theory and is similar to the proof of Theorem 3 and 4. By Theorem 5,

$\Xi_i^{[t,t+\Delta t]}$ is i.i.d. distributed and independent of x_i^t thus we can use the Boolean Model [19] to model the area that users have covered during $[t, t + \Delta t]$, i.e.,

$$\tilde{\Phi}_\Xi^{[t,t+\Delta t]} = \{(x_i^t, \Xi_i^{[t,t+\Delta t]})\}_i.$$

The set of users that has crossed channel x during $[t, t + \Delta t]$ is given by

$$N_{\mathrm{B}}^{[t,t+\Delta t]} = \{x_i : x_i \in \Phi, x_i^t + \Xi_i^{[t,t+\Delta t]} \cap x \neq \emptyset\}.$$

$|N_{\mathrm{B}}^{[t,t+\Delta t]}|$ is a Poisson random variable with parameter $\lambda \mathrm{E}[\nu_2(\check{x} \oplus \Xi_i^{[t,t+\Delta t]})]$, where ν_2 is the area of the set [19].

A_0 is bilateral symmetric, $\theta_i \sim \mathrm{unif}(0, 2\pi)$ and s_i is independent from θ_i, thus $\tilde{\Phi}_\Xi^{[t,t+\Delta t]}$ is isotropic. For isotropic $\Xi_i^{[t,t+\Delta t]}$ and Φ^t following HPPP with density λ, we have the following theorem for $\mathrm{E}[\nu_2(\check{x} \oplus \Xi_i^{[t,t+\Delta t]})]$.

Theorem 6. *K is a closed convex set and the typical grain Ξ_0 is convex and isotropic. In two dimensional case,* $\mathrm{E}[\nu_2(\check{K} \oplus \Xi_0)]$ *is given as follows,*

$$\mathrm{E}[\nu_2(\check{K} \oplus \Xi_0)] = \nu_2(K) + \mathrm{E}[\nu_2(\Xi_0)] + \frac{1}{2\pi} \nu_1(K) \mathrm{E}[\nu_1(\partial\Xi_0)], \tag{12}$$

where ν_1 is the one-dimensional measure and $\partial\Xi_0$ is the boundary of Ξ_0.

Theorem 6 is the 2-D case of the general result on the average number of grains hitting a convex set []. The proof involves integral geometry and generalized Steiner formula.

By Theorem 6 and make $K = x$, then we have

$$\mathrm{E}[\nu_2(\check{x}\oplus\Xi_0^{[t,t+\Delta t]})] = \mathrm{E}[\nu_2(\Xi_0^{[t,t+\Delta t]})] + \frac{|x|}{\pi}\,\mathrm{E}[\nu_1(\partial\Xi_0^{[t+\Delta t}])].$$

By geometry ananlysis, we have

$$\begin{aligned}\mathrm{E}[\nu_2(\Xi_0^{[t,t+\Delta t]})] &= \nu_2(A_0) + D_0\,\mathrm{E}[s]\Delta t,\\ \mathrm{E}[\nu_1(\Xi_0^{[t,t+\Delta t]})] &= \nu_1(A_0) + 2\,\mathrm{E}[s]\Delta t,\end{aligned}$$

where D_0 is the width of user's cross section along user's orientation.

Now we can compute the probability that channel x is not blocked as follows,

$$\begin{aligned}\mathrm{P}_{\mathrm{LOS}} &= \mathrm{P}(N_{\mathrm{B}}^{[t,t]} = 0)\\ &= e^{-\,\mathrm{E}[N_{\mathrm{B}}^{[t,t]}]}\\ &= e^{-\lambda(\nu_2(A_0)+\frac{|x|}{\pi}\nu_1(A_0))}.\end{aligned} \tag{13}$$

Armed with the analysis for the number of users that have blocked channel during any time interval, we now analyze the dynamics of the state of channel. We model channel x as a queue, Q, while the blockages are modeled as the jobs coming to the queue. The service time S is the time that a blockage blocks the channel. Since we assume that the movements of users are independent from each other, the time that each blockage blocks the channel (stays in the queue) is independent from others thus Q has infinite servers. For the number of new blockages (NB) that begin to block channel x during $[t, t+\Delta t]$, $N_{\mathrm{NB}}^{[t,t+\Delta t]}$, we have the following theorem.

Theorem 7. *For CVM, $N_{\mathrm{NB}^{[t,t+\Delta t]}}$ follows a Poisson distribution with density $\lambda\,\mathrm{E}[s](D_0 + 2|x|/\pi)$.*

Proof. The users that begins to block channel x during $[t, t+\Delta t]$ is an independent thinning of a PPP, thus $N_{\mathrm{NB}^{[t,t+\Delta t]}}$ follows Poisson distribution.

The number of users that begins to block the channel is the number of users that has blocked channel x during $[t, t+\Delta t]$ minus the number of blockages at t,

$$\begin{aligned}N_{\mathrm{NB}}^{[t,t+\Delta t]} &= N_{\mathrm{B}}^{[t,t+\Delta t]} - N_{\mathrm{B}}^{[t,t]}\\ \mathrm{E}[N_{\mathrm{NB}}^{[t,t+\Delta t]}] &= \mathrm{E}[N_{\mathrm{B}}^{[t,t+\Delta t]}] - \mathrm{E}[N_{\mathrm{B}}^{[t,t]}]\\ &= \lambda\,\mathrm{E}[s](D_0 + 2|x|/\pi)\Delta t.\end{aligned}$$

□

By Theorem 7, the arrival of blockages is memoryless. The time that u_i blocks the channel is related to x_i, θ_i and s_i. Given the above analysis, Q is a $M/GI/\infty$ queue, and the arrival rate of blockages, λ^Q is as follows,

$$\lambda^Q = \lambda\,\mathrm{E}[s](D_0 + 2|x|/\pi). \tag{14}$$

Let T_{LOS} be a random variable denoting the time a LOS link is available in steady state and T_{NLOS} be the time that the channel stays blocked. For $M/G/\infty$ queue, T_{LOS} follows a exponential distribution with parameter λ^Q, thus $\mathrm{E}[T_{\mathrm{LOS}}]$ is given by,

$$\mathrm{E}[T_{\mathrm{LOS}}] = \frac{1}{\lambda\,\mathrm{E}[s](D_0 + \frac{2|x|}{\pi})}. \tag{15}$$

The distribution of Q's busy period T_{NLOS} is difficult to derive and related to A_0 and the distribution of s, thus we focus on $\mathrm{E}[T_{\mathrm{NLOS}}]$ to see how user mobility influence the blocked period of the channel. The system is stationary thus we have the following relationship between $\mathrm{P}_{\mathrm{LOS}}$, $\mathrm{E}[T_{\mathrm{LOS}}]$ and $\mathrm{E}[T_{\mathrm{NLOS}}]$,

$$\mathrm{P}_{\mathrm{LOS}} = \frac{\mathrm{E}[T_{\mathrm{LOS}}]}{\mathrm{E}[T_{\mathrm{LOS}}] + \mathrm{E}[T_{\mathrm{NLOS}}]}. \tag{16}$$

From (16), we can derive $\mathrm{E}[T_{\mathrm{NLOS}}]$ as follows,

$$\mathrm{E}[T_{\mathrm{NLOS}}] = \frac{1-\mathrm{P}_{\mathrm{LOS}}}{\mathrm{P}_{\mathrm{LOS}}}\,\mathrm{E}[T_{\mathrm{LOS}}],$$

where $\mathrm{P}_{\mathrm{LOS}}$ is given in (13) and $\mathrm{E}[T_{\mathrm{LOS}}]$ is given in (15).

Based on the results of $\mathrm{E}[T_{\mathrm{LOS}}]$ and $\mathrm{E}[T_{\mathrm{NLOS}}]$, we can compute the frequency that the state of channel changes from LOS to NLOS then back to LOS, f_{change}, as follows,

$$f_{\mathrm{change}} = \frac{1}{\mathrm{E}[T_{\mathrm{LOS}}] + \mathrm{E}[T_{\mathrm{NLOS}}]}.$$

In some cases we can get more information about the distribution of T_{NLOS}. If the time that each user blocks the channel is equal, e.g., all users have the same orientation and velocity, Q becomes an $M/D/\infty$ queue and the distribution of busy period is given in [20]. The author of [20] also shows that the busy period of $M/GI/\infty$ queue is asymptotically exponential with mean equal to expected busy period if the distribution function of service time, H, satisfies that,

$$(\log z)\int_z^\infty \{1 - H(y)\}\mathrm{d}y \to 0, \tag{17}$$

as $z \to \infty$. For our constant velocity model, we derive a sufficient condition for busy period to approximate exponential distribution in the following theorem.

Theorem 8. *For CVM, the distribution of T_{NLOS} approximates exponential distribution with mean $\mathrm{E}[T_{\mathrm{NLOS}}]$ if the velocity of blockages meets following condition,*

$$s_i \geq s_{\min}, s_{\min} > 0, \tag{18}$$

for all blockages i.

Proof. $s_i > s_{\min}$ then service time S_i is bounded by $(|x| + d_A)/s_{\min}$, where d_A is the diameter of the smallest circle that cover contains A. $H(y) = 1$ for $y > (|x| + d_A)/s_{\min}$ thus (17) is satisfied. By Theorem 1 in [20],

$$\mathrm{P}(\mathrm{E}[T_{\mathrm{NLOS}} \leq z\,\mathrm{E}[N_{\mathrm{NLOS}}]]) \to 1 - e^{-z}, z > 0,$$

as $\lambda^Q \to \infty$. □

Theorem 8 indicates that the exponential distribution is a good approximation for T_{NLOS} if λ^Q is large. From (14), we know that λ^Q is large if user density is high, user speed is large and channel x is long. [21] provides some other conditions when the distribution of busy period is approximately exponentially distributed.

If λ^Q is small, exponential distribution may not fit T_{NLOS} well. For example, if λ^Q is very small, the probability that the channel is blocked by more than one blockage is small and the distribution of T_{NLOS} can be approximated by the distribution of S.

Coupling of blockages?

III. Numberical Results for Interference Environment and Implications on MAC design

In this section, we show the numerical results for our analysis in Section II and discuss the implications of the interference environment on MAC design.

We first compute $\mathrm{E}[N_{\mathrm{SI}}]$ for simple user body model, in which we model users as cylinders with a diameter of 0.6 m. We then compare the analytical results with simulations. In dense environment, the volume of human body is not negligible and the distribution of users will be more organized as user density increases since there will be some minimum distance between users. To evaluate how much this factor affects our the accuracy of our analysis, we use Matérn III process [22] to model the locations of users and instead of HPPP. The height of users is 1.754 m, and the height of the ceiling is 2.8 m. The material of the ceiling is one layer polyester board with a thickness of 9 mm. We assume the users do not have a specific polarization. $r_{\max} = 10$ m, at which distance the path loss of LOS channel is -88 dB, and $r_{\max}^{\text{reflection}} = 3$ m.

In Fig. 4 we show $\mathrm{E}[N_{\mathrm{SI}}]$ for different user densities. The average number of LOS and NLOS interferers are exhibited and compared to the results from simulations. In the simulation, we place the device on the surface of user body and adjust (10) accordingly. Our analytical results are in line with the simulations, validating the accuracy of the approximation.

As can be seen, $\mathrm{E}[N_{\mathrm{SI}}]$ first grows in the user density, but as user density further increases, users closely around the typical user form a ring blocking the interference from most users outside the ring. Also note that users see the most strong interferers at moderately high user densities.

Fig. 5 illustrates how the distribution for the distance of strong interferers for varying user densities, with self blockage not considered. In high density scenario, the number of users the MAC needs to coordinate is actually limited, indicating that it is possible to mitigate interference in highly dense scenario using local coordination among users.

Next we compute the sensitivity of users at different distance when users only make local movements. We only consider LOS strong interferers in our evaluation. The movements of users during Δt is as follows, Δx is uniformly distributed in a disc centered at the origin with the radius of $r(\Delta t)$, $\Delta x \sim \mathrm{unif}(\mathcal{B}(0, r(\Delta t)))$, and $\Delta\theta$ is uniformly distributed

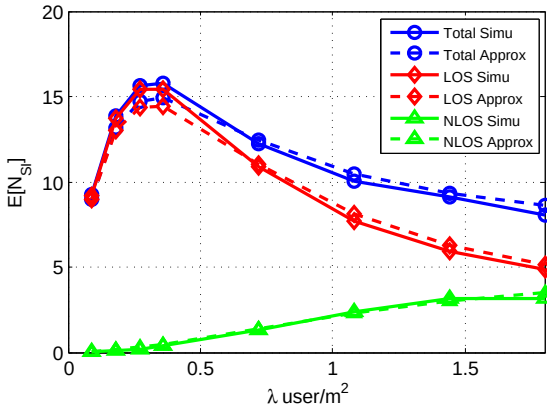

Fig. 4. $\mathrm{E}[N_{\mathrm{SI}}]$ for different user densities. Whether user at x' blocks the channel is decided by $h_x(x', \theta')$ and h_{NLOS}.

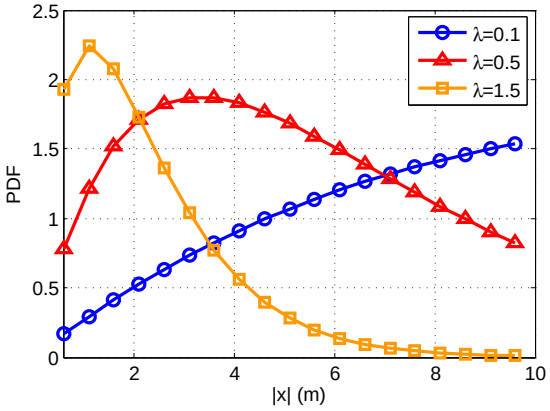

Fig. 5. Probability density function of LOS strong interferers as a function of the distance to the typical user at $\mathbf{0}$.

in an interval, i.e., $\theta \sim \mathrm{unif}[-\omega(\Delta t), \omega(\Delta t)]$. The range of translations of users is related to user density, when λ is small, Δx is independent of λ; if λ is high, Δx decreases as λ increases. In our simulation, $\Delta t = 1$s. How r changes with λ is plotted in Fig. 6 and $\Delta\omega = 24°$.

In Fig. 7, we exhibit the sensitivity of users at different locations. Distant interferers are more sensitive to perturbations than close by interferers. This supports the observation

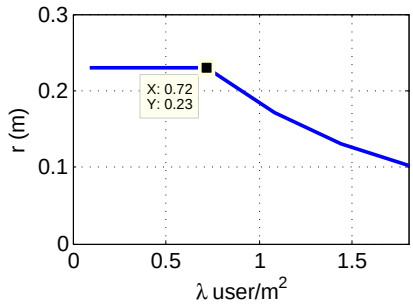

Fig. 6. Range of translation r for different user densities λ. For low user density, $\lambda < 0.72$, r is fixed. For large λ, $r = 0.6\sqrt{1/\lambda\pi}$ for $\lambda > 0.72$.

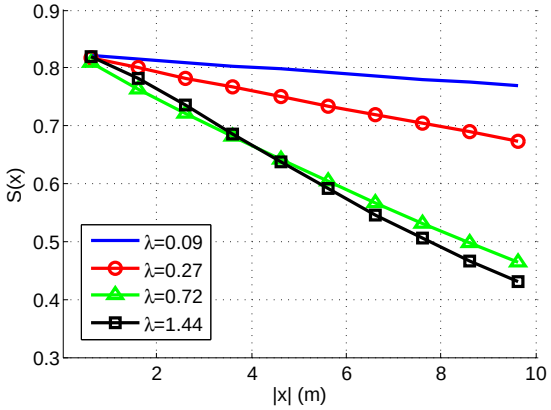

Fig. 7. Sensitivity of users at different distances $|x|$.

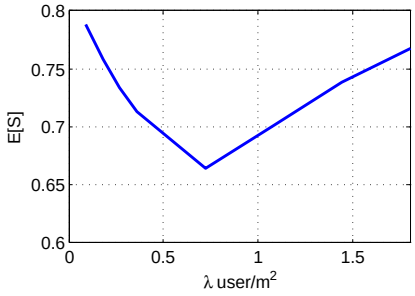

Fig. 8. $\mathrm{E}[S(x)|f_0(x_i,\theta_i,\tilde{\Phi}\backslash\{(x_i,\theta_i)\},\theta_0) = 1]$ average sensitivity of strong interferers.

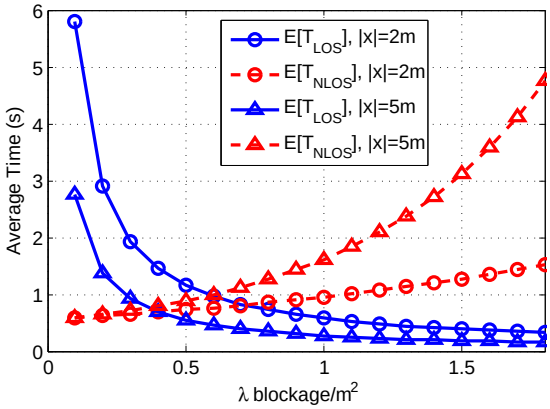

(a) $\mathrm{E}[T_{\mathrm{LOS}}]$ and $\mathrm{E}[T_{\mathrm{NLOS}}]$

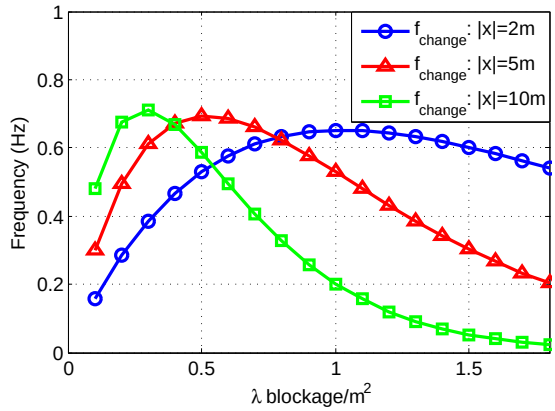

(b) State change frequency f_{change}

Fig. 9. $\mathrm{E}[T_{\mathrm{LOS}}]$, $\mathrm{E}[T_{\mathrm{NLOS}}]$ and f_{change} for different λ and $|x|$. User's average velocity is $\mathrm{E}[s] = 1$m/s. Blockage is modeled as a rectangle of size $0.45\mathrm{m} \times 0.25\mathrm{m}$ and the width towards moving direction is $D_0 = 0.45\mathrm{m}$.

that clusters compromising closeby nodes (interferers) will be robust to perturbations and learning the interference form close by neighbors is more reliable.

Fig. 8 exhibits how the average sensitivity of strong interferers changes for different user densities. When user density increases, strong interferers are closer while the sensitivity of users decreases, thus the average sensitivity first decrease in the As the density of users continues to increase, this limits their range of translation and the sensitivity of users remains the same while $\mathrm{E}[S]$ increases as strong interferers are more likely to be close to the typical user.

The above results show that interferers are more sensitive to perturbation, and thus harder to keep track of as user density increases and the worst case happens in the moderately high user density scenario, where the number of strong interferers is high and the range of perturbation is not limited by the density of users.

In Fig. 9 we present how $\mathrm{E}[T_{\mathrm{LOS}}]$, $\mathrm{E}[T_{\mathrm{NLOS}}]$ and f_{change} changes for different blockage density λ and channel lengths $|x|$. From (15) we know that $\mathrm{E}[T_{\mathrm{LOS}}]$ is inversely proportional to $\lambda\,\mathrm{E}[s]|x|$ if we ignore D_0. Results in Fig. 9(a) indicate that if the blockage density is higher, the blockages move faster and the link is longer, then the time of having LOS channel decreases while the time of having NLOS channel increases. Results in Fig. 9(b) indicate that the state of channel changes most frequently at moderately high user densities. In dense wearable networks, distant users are likely to be blocked and state of their channel is relatively stable thus we may ignore theses users in MAC protocol.

IV. Clustering and Channel Selection in Dense Wearable Networks

V. Analysis of Clustering

VI. Conclusion

VII. Clustering and Channel Selection

Clustering improves spatial reuse and reduce interference [2]. Cluster head synchronizes the cluster members and schedules beacon transmissions in the cluster to mitigate intra-cluster interference, while other techniques like channel selection (FDM) and back off [24] can be used to reduce inter-cluster interference. The 802.11ad Standard provides both distributed clustering and centralized clustering methods for directional devices working on mmWave. The links between PCPs/APs are unstable in dense wearable networks, thus the distributed clustering method fits better and we will use the distributed clustering algorithm in 802.11ad as the baseline.

In the distributed clustering algorithm, the formation of cluster follows a first come first serve rule: a BSS tries to join a existing cluster when it enters a network and starts a new cluster if no existing cluster is available. The maintenance of clusters is similar to lowest ID clustering. If the original cluster head is lost or two clusters meet each other, the remaining BSS or the original cluster head with the lowest/lower ID will be selected as the new cluster head. The Beacon SPs of cluster members are non-overlapping in time and a BSS need to reserve the slots if the PCP/AP or other devices receive beacons or Extended Schedule element from other BSSs. Distributed clustering help schedule beacon transmissions and the BSSs share the channel in a pure TDMA way.

In dense wearable networks, the TDMA like scheduling method based on omni-directional beacons will not allocate enough resource for BSSs and channel reuse is necessary. Furthermore, the channels between devices, especially the channels between PCPs/APs of cluster members and PCPs/APs of cluster heads, are unstable, leading to frequent lost of cluster heads and reforming of clusters. A good clustering should cluster BSSs that have stable connections to cluster heads and facilitate resource reuse at BSS level.

The requirements of clustering are affected by the network scenario. If users move a lot, e.g., users getting off a subway train car or moving along the aisle, the channels changes fast and the basic requirements of clustering algorithm is to be fast in formation and maintenance. If users moves locally and are relatively stable, clusters can be optimized to form more stable clusters so that BSSs can better schedule their transmissions by learning their interference environment.

Choosing the proper size of clusters is important for dense wearable networks. Big clusters can reduce inter-cluster interference but a cluster would reserve more slots for beacon transmission and the slots for each BSS's primary high-end transmission is limited. Furthermore, the connections between cluster members and cluster heads can be unstable. Small clusters provide enough resource for each cluster member and are easy to maintain but suffer from more inter-cluster interference.

Another question with wearable network clustering is what devices should participate in clustering. Devices of the same BSS are controlled by PCP/AP and communicate with each other thus BSS is the basic unit in clustering. However, the interference environments of different devices can be completely different due to the short wave length and human body shadowing. Choosing the devices to participate in clustering requires the trade-off between the accuracy of channel estimation and the cost for measurement and signaling. The PCPs/APs send beacons in every slot and PCPs/APs within the same cluster are required to listen to the beacons thus the channel between PCPs/APs are measured in every frame. The non-PCP/non-AP devices can measure the channel from PCPs/APs by listening to the beacons, but the measurements cost energy and the measurements need to be sent to PCP/AP. The measurement of channels from non-PCPs/non-APs will require additional pilots. In our case, the connectivity between cluster members and cluster heads require measurements and message exchange between PCPs/APs thus PCPs/APs are necessary in clustering. The high-end non-PCP/non-AP devices can measure the interfering channel from other PCPs/APs and send the results to PCP/AP to improve clustering. Low-end devices have limited energy thus they are not required to measure interference. Optimization of clusters also requires the measurements and exchange of control messages between BSSs working on different channels thus BSSs need to measure other channels and exchange messages periodically.

Our purpose here is to devise a clustering algorithm to provide stable clusters where the connections between cluster heads and cluster members are more stable and use a channel selection algorithm to further reduce inter-cluster interference.

A. Clustering based on Affinity Propagation

Affinity Propagation (AP) [25] is a distributed clustering algorithm which elects a set of exemplars and assign nodes to exemplars based on message exchange between nodes . AP clustering maximizes the sum of pairwise similarities between nodes and their exemplars, where similarity $s(i,k)$ indicates how well node k serves as the exemplar of node i. The clustering result does not depend on the initialization of cluster heads and only requires exchange of real value messages between data nodes and AP clustering can produce good clustering result at low computational and signaling cost compared to other clustering techniques such as k-centers clustering.

In AP clustering, nodes exchange two types of messages and the messages are combined to decide cluster heads and association. Each node i sends 'responsibility' $r(i,k)$ to candidate cluster head k, indicating how suitable node k works as node i's cluster head compared to other candidate cluster heads. The candidate cluster head k sends 'availability' $a(i,k)$ to node i to show the accumulative support for being a cluster head that node k receives from nodes other than i. The messages are initialized to be 0 and messages of the same type are updated at the same time.

The responsibilities are computed as the similarity minus the maximum of the sum of availability and similarity of other competing cluster heads,

$$r(i,k) = s(i,k) - \max_{k' \text{s.t.} k' \neq k} \{a(i,k') + s(i,k')\}. \qquad (19)$$

The candidate cluster heads compete for the ownership of node i and the candidate cluster head with larger similarity value compared to other potential cluster heads is more likely to own node i. For $i = k$,

$$r(i,i) = s(i,i) - \max_{k \text{s.t.} k \neq i} \{a(i,k) + s(i,k)\}$$

is the self-responsibility for becoming a cluster head and $s(i,i)$ is the prior preference for being a cluster head. A negative self-responsibility means the node is better working as a cluster member instead of a cluster head. If $s(i,i)$ is large, BSS i will tend to start its own cluster and the density of cluster heads will increase; otherwise, the clustering algorithm will produce fewer cluster heads and larger clusters.

The availabilities are computed at the candidate cluster heads by adding self-responsibility and the positive responsibilities they receive from other nodes:

$$a(i,k) = \min\left\{0, r(k,k) + \sum_{i' \text{s.t.} i' \neq i,k} \max\{0, r(i',k)\}\right\} \quad (20)$$

$$a(k,k) = \sum_{i' \text{s.t.} i' \neq k} \max\{0, r(i',k)\} \quad (21)$$

A candidate cluster head with stronger support from other nodes and high self-responsibility is more likely to become a cluster head and the availability is high.

At any stage, the messages can be combined to decide the cluster heads. The nodes which have positive sum of self-availability and self-responsibility will be elected as cluster heads, i.e., $CH = \{k | a(k,k) + r(k,k) > 0\}$. Other nodes select the cluster head which maximize the sum of availability and responsibility:

$$ch(i) = \arg\max_{k \in CH} \{a(i,k) + r(i,k)\}, \forall i \notin CH.$$

However, there is no guarantee of convergence for AP clustering. To avoid numerical oscillations and reach convergence, the messages need to be damped when updated, e.g., $m(t+1) = (1-\lambda)m(t) + \lambda m$.

AP-based clustering algorithms have been proposed to produce stable clusters [26] or reduce signaling overhead[27]. In our case, we want cluster members to have stable connections to cluster heads and reduce inter-cluster interference. The stability of channels is inferred by tracking the channel quality over time. To get stable channels between users, a good 'similarity' metric would be the 'stability' of channel and we use the average channel strength to measure stability,

$$Stability(i,j) = Pr(|H_{i,j}|^2 > \gamma),$$

where $H_{i,j}$ is the record of estimations of channel gain from PCP j to PCP i in previous frames. To mitigate inter-cluster interference and facilitate the exchange of messages within cluster, cluster members should share similar strong interferers with the cluster head so that inter-cluster interference can be effectively reduced by making neighbor clusters work on different channels. We devise a metric to measure the similarity in strong interfering neighbors, *Common Neighbor Stability* (CNS). CNS between two BSSs is defined as the sum of minimum of the two BSSs' stability to their common interfering neighbors, i.e.,

$$CNS(i,j) = \sum_{k \in N_i} \min(Stability(i,k), Stability(j,k)). \quad (22)$$

N_i is the set of most stable strong interferers of BSS i, $|N_i| = M$. BSS i broadcasts N_i and corresponding $Stability(i,:)$ in its beacons or clustering messages periodically and BSSs hearing the beacons update their CNS to BSS i. CNS is computed locally at each BSS and the set N varies for different BSSs thus CNS can be asymmetric, i.e., $CNS(i,j) \neq CNS(j,i)$. $Stability(i,i) = 1$ by default. We use CNS as the similarity metric for AP clustering to elect the exemplars and when a BSS decides to join a cluster, it selects the cluster head which has best stability and CNS, i.e.,

$$CH(i) = \arg\max_k \{Stability(i,k) \cdot CNS(i,k)\}.$$

Running AP clustering for a network consisting of N BSSs has a signaling complexity of $O(N^2)$. However, the actual signaling cost can be reduced to $O(N)$. Only positive responsibilities are needed thus a node only need to broadcast positive responsibilities in its beacons. For availabilities, node k just need to broadcast $a(:,k) = r(k,k) + \sum_{i' \text{s.t.} i' \neq k} \max\{0, r(i',k)\}$ to other nodes, and node i can update $a(i,k)$ as $a(i,k) = \min(0, a(:,k) - \max(0, r(i,j)))$. Furthermore, we do not need to assign non-overlapping slots for signaling: if two BSSs can hear each other, they will reserve slots for the beacon transmission of each other; if two BSSs do not have a good connection, then they are not likely to become the cluster head of the other BSS and the message exchange is not necessary. Applying AP clustering only requires each BSS to broadcast limited messages in their beacons thus the signaling over head is limited.

We use channel selection to reduce inter-cluster interference. Channel selection is performed by the cluster head to avoid using the same channel as its stable strong interferers. The PCP/AP of cluster head estimates the channels to nodes outside the cluster periodically. If the inter-cluster interference is high, the cluster head may switch to another channel with certain probability. The cluster head then estimates the interference environment on the new channel for some slots and decide to stay on the new channel or switch back to the original one based on measurements. If the network is stable, such channel selection method can assign neighboring clusters to different channels and reduce inter-cluster interference.

B. Analysis of Clustering Performance

The major variant in our clustering algorithm is cluster size. In dense wearable networks, small clusters provides more parallelism across clusters but users experience more inter-cluster interference; large clusters reduce inter-cluster interference but the resource reserved for each user is limited and the it is more difficult to maintain connections between cluster heads and cluster members. In this part we analyze

the throughput of users for different network scenarios and assumptions about users and try to identify the optimal cluster size.

To model the clusters, we assume the cluster members

C. Clustering Results

We apply AP based clustering algorithm and channel selection in dense scenario. We use Markov Contention Matrix to model the channel between different users in Section II. For comparison, we also simulate lowest ID clustering, which is a simplified version of the distributed clustering algorithm used in 802.11ad. We evaluate the performance of the clustering algorithms using two metrics, the average probability of having LOS channel with cluster heads and the average number of LOS interferers working on the same channel within the cluster and outside the cluster. The clustering results are shown in Fig. and Table We can see that AP based cluster can effectively cluster the nodes that are close in proximity (well-connected) and channel selection effectively reduce the number of LOS interferers. In fact, lowest ID clustering provides fewer strong interferers, but the cluster heads and the cluster members are not well connected thus the signaling within the cluster is hard to perform. Furthermore, the number of uncoordinated LOS interferers is not reduced (if not increased). If we only perform channel selection without clustering, the average number of total LOS interferers is also smaller, but the interference is uncoordinated and more unpredictable.

Our AP based clustering algorithm requires frames scheduled for channel measurements and message exchange for BSSs working on different channels. This will introduce extra signaling cost thus we are working on devising pure distributed clustering algorithm and channel selection only relying on message exchanging on the same channel.

VIII. Hierarchical MAC Scheduling for Heterogeneous Devices

With appropriate clustering and channel selection, we can form clusters that are in close proximity. The above approach does not remove inter-cluster interference completely, but the interferers from outside the cluster are more distant away thus the set of inter-cluster interferers are less stable as shown in Fig. The interfering channel to inter-cluster interferers are likely to be blocked, making learning the transmission patterns of BSSs outside the cluster ineffective. A simple way to deal with interference is to treat interference as noise. If inter-cluster interference is strong, the BSS may consider switching to another cluster or work on another channel.

After performing channel selection, the average number of strong interferers working on the same channel would be approximately $1/M$ of the average number of total strong interferers, M being the total number of channels. Such number is relative small, however, simple TDM scheduling used in 802.11ad is not enough. In 802.11ad, a PCP/AP would reserve the slots for other BSSs if the PCP/AP or the non-PCP/non-AP devices receives the extended schedule element of other BSSs. The set of strong interferers may change fast over time, thus the number of Extended Schedule Element a BSS receive. As a result of it, there can be much more BSSs working in the same contention group. If instead, all BSSs do not reserve resource for neighbor BSSs, interference will be unpredictable, making it hard to guarantee the QoS of transmission.

As discussed in Section **??**, high-end and low-end devices have different QoS requirements and transmission capabilities. A basic principle with the MAC design is that high-end devices should work on reserved slots. BSSs would reserve the slots for the high-end transmissions to avoid degrading the QoS. For low-end devices, or not important high-end transmissions, BSS try to reuse the slots of other BSSs' high-end transmission by first sensing the channel. Due to the energy limit of low-end devices, channel sensing may not be performed in all slots. To effectively sensing and reusing the channel, low-end devices can stay idle for some time if there is interference on the channel it try to reuse or select the slot that are more likely to be idle to work on.

To apply the MAC principle, we first model the contention relationship in dense wearable network using Markov model. The channel between two BSSs, i and j, is modeled as a discrete Markov process with two states. If there is a LOS channel, or strong reflection channel between i and j, the state of channel is 0; the state is 1 otherwise. The channel state transits in each frame and the state transition diagram is shown in Fig. The state transition rate is determined by the users density, the movement pattern of users and the length of the channel.

We begin with a toy example, optimizing the reward from scheduling secondary transmission. For a slot in which a BSS works as a secondary user, the BSS can take three actions, Transmit, Sense and Idle. The reward of a successful transmission is R_{Transmit}, and the energy cost using different states is E_{Transmit}, E_{Sense} and E_{Idle}. The corresponding state transition matrix is shown in Fig. The optimization problem can be solved as a Markov Decision Process, which optimize the discounted sum of potential gain over time. Another objective is to optimize the average reward over frames. As shown in Fig. the optimization problem involves two decisions, the number of slots to wait if the channel is sensed to be interfered and the action to take after waiting. For different decisions, the stationary distribution of states and corresponding reward over time. Let k be the number of slots that a BSS stays idle after the channel is interfered by the primary user, $k = \{0, 1, \dots, \}$. There are three states, *Transmit*, *Idle* and *Action*. *Action* is the state that a BSS either transmit or sense the channel after staying idle. The stationary distribution of the state is as follows,

$$\begin{aligned} \pi_{Transmit} &= \frac{P(0| < k+1 >)}{P(0| < k+1 >) + 2 \cdot p_{block}} \\ \pi_{Idle} &= \frac{p_{block}}{P(0| < k+1 >) + 2 \cdot p_{block}} \\ \pi_{Action} &= \frac{p_{block}}{P(0| < k+1 >) + 2 \cdot p_{block}} \end{aligned} \tag{23}$$

State *Idle* takes k frames while the other two states take one frame. Given the stationary distribution of states, we can compute the average gain over time for different combination of k and action taken after waiting. A BSS can treat each slot independently and optimize the reward from each slot. However, there is limitation with the above approach. The first problem is that the secondary users might interfere with each other thus the reward from utilizing a slot is not constant. If the BSSs try to reuse the slots aggressively, there will be more interference among the secondary users thus reducing the gain of reuse. The second limitation with the naive approach is that the QoS requirements are not fully considered. The rewards of different slots in a frame are correlated. A BSS will not always have data to transmit but may have different requirements on delay. If a BSS reuse multiple slots of a frame successfully and does not have more data to transmit, the reward from reusing a new slot will be trivial, even negative. On the other hand, if the BSS does not have enough slots, a BSS should probe/transmit more aggressively to meet the QoS requirements. The third limitation is the exact optimization requires the exact channel between primary and secondary BSSs. To deal with this problem, a BSS can adjust its decision making procedure according to the results from the channel. If a slot is constantly busy, BSS can increase the time of staying Idle; otherwise, the time of waiting can be shortened. In fact, the analytical results in Fig. supports the philosophy of adaptation: the long channels are more likely to be blocked by obstructions and interference from far away neighbors are more likely to be blocked due to the movements of users, thus the channels that are often blocked are more likely to become blocked after certain frames.

Considering the above discussed limitations, we extend the hierarchical scheduling to optimize the resource a BSS can get from reusing slots in one whole frame. Each frame consists of N slots, and there are N BSSs working in one cluster. At the beginning of each frame, the PCP/AP node broadcast Beacons to the non-PCP/non-AP nodes and the schedule for the frame is contained in the Beacon, thus a BSS need to make the scheduling decisions at the beginning of each slot based on the measurements in the previous frame and can not schedule new transmissions during the frame. For a typical BSS, the state of a frame is as follows,

$$FrameState = \{SlotState_1, SlotState_2, \ldots, SlotState_N\}.$$

$SlotState_i$ is the same as the slot state used for toy example. In our design, Slot 1 is the slot reserved for primary transmission. Ignoring inter-cluster interference, the BSS does not need to consider $SlotState_1$ in scheduling. We assume the channels between the BSS and other BSSs are independent from each other, thus the state transition diagram of each slot is the same as shown in Fig. The difference is that the reward on a slot is also influenced by the interference from other BSSs in the same cluster and the QoS requirements of the BSS. Assuming the BSSs are independent from each other and all the channels between any pair of BSSs are independent from each other and the transition for each link are identical, then intra-cluster interference is a function of the probability that a slot schedules transmission. For the QoS requirements of BSSs, the marginal gain from reusing the slot decreases with the slots available to the BSS. Considering intra-cluster interference explicitly makes the reward influenced by the decision that the BSS makes for different states, thus the standard MDP procedure no longer works. To solve such problem, one method is update the values and decisions of different states iteratively while updating the reward of state transition over iteration. The second method is to solve the problem by brute force search over the whole state space.The problem with such approach is that the size of the state space is very large. Even we limit the number of frames that a BSS would stay idle to be a limited number, e.g., M, the size of state space is $(M+2)^N$.

The computational complexity with MDP approach is not affordable thus we need to find heuristic scheduling methods for reusing the MAC, which strike a balance between simple naive scheduling over each slot and the optimization over all the potential state space. Two major objectives of heuristic scheduling includes 1) reuse slots based on measurements of channel in previous frames without knowing the exact parameter of the channel and 2) making each BSS to have some slots to work on to meet minimum QoS requirements and achieve fairness among secondary BSSs. To serve the above two objectives, the key idea of our scheduling methods is that each BSS schedule transmissions on slots where there is no interference from primary users while keeping track of an additional slot with no interference. If the channel to the primary BSS does not change, the BSS will keep using the slot; otherwise the BSS try to reuse the alternative slot instead. The detailed scheduling algorithm is as follows.

In each slot, a BSS has the channel measurements from the previous frame. There will be some slots in which a BSS does not see interference from primary users. The BSS selects K available slots to schedule its secondary transmission and keeps track of an alternative slot in case one of the reused slots is no longer available. The BSS will always have the measurements of the slots that they schedule secondary transmission. To keep track of the alternative slot, the BSS schedule $Sense$ on one of the rest of the slots. If the slot is sensed as available, it is an alternative slot and the BSS may either keep sensing that channel or sensed that channel again after some time, based on the variability of the channel. If the BSS sees interference from the primary user, it reschedule its secondary transmission on the alternative slot and scheduling sensing on the slot which has the highest probability of having no interference from primary users among the rest of the slots. If more than one slot reused become unavailable, the BSS reschedule transmissions on the slots with highest probabilities of not having interference from primary BSSs. At the same time, the BSS schedule sensing on the other slots.

IX. Simulation Evaluation

X. Conclusion

References

[1] "Smart Wearable Devices: Fitness, Glasses, Watches, Multimedia, Clothing, Jewellery, Healthcare & Enterprise 2014-2019," *Juniper Research*, Aug. 2014.

[2] *"IEEE Standard for Information Technology Telecommunications and Information Exchange between Systems Local and Metropolitan Area Networks Specific Requirements. Part 11: Wireless MAN Medium Access Control (MAC) and Physical Layer (PHY) Specifications Amendment 3: Enhancements for Very High Throughput in 60 GHz Band,"*, IEEE Standard 802.11ad, 2012.

[3] *"IEEE Standard for Information Technology Telecommunications and Information Exchange between Systems Local and Metropolitan Area Networks Specific Requirements. Part 15.3: Wireless Medium Access Control (MAC) and Physical Layer (PHY) Specifications for High Rate Wireless Personal Area Networks (WPANs) Amendment 2: Millimeter-Wave-Based Alternative Physical Layer Extension,"* IEEE Std 802.15.3c, 2009.

[4] *"High Rate 60 GHz PHY, MAC and PALs,"* ECMA Standard 387, 2010.

[5] S. Y. Geng, J. Kivinen, X. W. Zhao, and P. Vainikainen, "Millimeter-wave propagation channel characterization for short-range wireless communications," *IEEE Trans. Veh. Tachnol.*, vol. 58, no. 1, pp. 3-13, Jan. 2009.

[6] C. Gustafson and F. Tufvesson, *"Characterization of 60 GHz Shadowing by Human Bodies and Simple Phantoms, "* Antennas and Propagation (EUCAP), 6th European Conference on, 2012.

[7] T. Bai and R.W. Heath Jr., "Coverage and rate analysis for millimeter wave cellular networks," in *IEEE Trans. Wireless Comm.*, vol. 13, no. 9, Sep. 2014.

[8] K. Venugopal, M.C. Valenti and R.W. Heath, *"Interference in Finite-Sized Highly Dense Millimeter Wave Networks,"* Information Theory and Applications Workshop, Feb. 2015.

[9] G. George and A. Lozano, "Performance of enclosed mmWave wearable networks," in IEEE Int'l Workshop on Compuational Advances in Multi-Sensor Adaptive Processing (CAMSAP 15), Dec. 2015. (Revision required)

[10] S. Collonge, G. Zaharia and G.E. Zein, "Influence of human activity on wide-band characteristics of the 60 GHz indoor radio channel," *IEEE Trans. Wirel. Commun.*, vol. 3, no. 6, pp. 2369-2406, 2004.

[11] S. Singh, F. Ziliotto, U. Madhow, E. M. Belding and M. Rodwell, "Blockage and Directivity in 60 GHz Wireless Personal Area Networks: From Cross-Layer Model to Multihop MAC Design," *IEEE J. Sel. Areas Commun.*, vol. 27, no. 8, Oct. 2009.

[12] I. Kashiwagi, T. Taga and T. Imai, "Time-varying path-shadowing model for indoor populated environments," *IEEE Trans. Veh. Technol.*, vol. 59, no. 1, Jan. 2010.

[13] C. Sum, Z. Lan, R. Funada, J. Wang, T. Baykas, M. A. Rahman, and H. Harada, "Virtual time-slot allocation scheme for throughput enhancement in a millimeter-wave multi-Gbps WPAN system," *IEEE J. Sel. Areas Commun.*, vol. 27, no. 8, Oct. 2009.

[14] L. X. Cai, L. Cai, X. Shen, and J. Mark, "REX: a randomized exclusive region based scheduling scheme for mmWave WPANs with directional antenna," *IEEE Trans Wireless Commun.*, vol. 9, no. 1, pp. 113-121, Jan. 2010.

[15] I. K. Son, S. Mao, M. X. Gong, and Y. Li, "On frame-based scheduling for directional mmWave WPANs," in *Proc. IEEE INFOCOM*, Orlando, FL, 2012, pp. 2149-2157.

[16] E. Shihab, L. Cai, and J. Pan, "A distributed asynchronous directional-to-directional MAC protocol for wireless ad hoc networks," *IEEE Tans. Veh. Tech.*, vol. 58, no. 9, pp. 5124-5134, Nov. 2009.

[17] S. Singh, R. Mudumbai, and U. Madhow, "Distributed coordination with deaf neighbors: efficient medium access for 60 GHz mesh networks," in *Proc. IEEE INFOCOM*, San Diego, CA, 2010, pp. 1-9.

[18] K. Sato *et al.*, "Measurements of Reflection and Transmission Characteristics of Interior Structure of Office Building in the 60-GHz band," *IEEE Trans. Antennas Propag.*, vol. 45, no. 12, pp. 1783-1792, Dec. 1997.

[19] F. Baccelli and B. Blaszczyszyn, "Stochastic geometry and wireless networks, volume I - theory," *Foundations and Trends in Networking*, vol. 3, no. 3-4, pp. 249-449, 2009.

[20] P. Hall, "Heavy Traffic Approximations for Busy Period in an M/G/∞ Queue," *Stochastic Processes and their Applications*, vol. 19, no. 2, pp. 259-269, 1985.

[21] M. A. M. Ferreira and M. Andrade, "The M/G/∞ Queue Busy Period Distribution Exponentiality," *Applimat - Journal of Applied Mathematics*, vol. 4, no. 3, pp. 249-260, 2011.

[22] B. Matérn, Spatial Variation second ed. vol.36 of Lecture Notes in Statistics. (Revision required)

[23] J. F. C. Kingman, "Poisson Processes," New York: The Clarendon Press Oxford Univ. Press, 1993.

[24] H. Lee, H. Kwon, A. Motskin and L. Guibas, *"Interference-aware MAC Protocol for Wireless Networks by a Game-Theoretic Approach,"*, in *INFOCOM*, Rio de Janeiro, 2009, pp. 1854-1862.

[25] B.J. Frey and D. Dueck, *"Clustering by Passing Messages Between Data Points,"* Science 315 (2007) 972-976.

[26] B. Hassanabadi, C. Shea, L. Zhang and S. Valaee, *"Clustering in Vehicular Ad Hoc Networks using Affinity Propagation,"* Ad Hoc Networks 13 (2014) 535-548.

[27] D.J. Son, C.H. Yu and D.I Kim, *"Resource Allocation based on Clustering for D2D Communications in Underlaying Cellular Networks,"* in *Information and Communication Technology Convergence*, Busan, 2014, pp. 232-237.